

FAILURE MODES OF PVD COATINGS IN MOLTEN Al-ALLOY CONTACT

Massimo Lorusso¹⁾, Daniele Ugues^{1)*}, Cristiana Oliva¹⁾, Rudy Ghisleni²⁾

¹⁾Politecnico di Torino, Department of Applied Science and Technologies, Torino, Italy

²⁾EMPA – Swiss Federal Laboratories for Materials Testing and Research, Laboratory for Mechanics of Materials and Nanostructures, Thun, Switzerland

Received: 25.09.2012

Accepted: 27.11.2012

*Corresponding author: daniele.ugues@polito.it; Tel. +39 011 0904705; Department of Applied Science and Technologies, Politecnico di Torino, Cso Duca degli Abruzzi, 24, 10129, Torino, Italy

Abstract

This paper deals with a study of the failure mode of thin PVD coatings in alternated contact with molten aluminum alloy. CrN and ZrN monolayer coatings deposited through cathodic arc evaporation were used. The coatings morphology was assessed by SEM and their mechanical properties evaluated by nanohardness test performed at room temperature. An experimental test rig which cyclically immerses coated steel samples in molten Al-alloy and in a cooling bath was applied. The thermal gradient from the coating to the steel core was exalted by internal cooling channels placed in the internal cavity of samples. Periodical SEM inspections were performed to assess the damaging levels introduced by the test and to study the related decrease of substrate protection capability. Descriptions and interpretations of the damages evolutions were derived. The main conclusions achieved are that both coatings suffered by the formation of corrosion pits, which were due to a corrosion attack of the steel substrate localized at coating defects sites. In particular, at pores locations the corrosion was fast, whereas at droplets sites it required a certain incubation time. Once corrosion pits were formed they exhibited an initial tendency to expand laterally, but they did rapidly stabilize in terms of lateral dimensions. Later on two different failure modes acted in ZrN and in CrN. Extended delamination due to a marked mismatch of mechanical properties between the coating and the steel substrate developed in ZrN. On the contrary, thermal cracking due to lower hardness levels developed in CrN, but with limited delamination. Accordingly the steel substrate protection capability was evaluated to be higher in CrN than in ZrN.

Keywords: PVD coating, die casting, corrosion pits, thermal cracking, delamination, failure modes

1 Introduction

The continuously developing research on vapour deposition technologies allowed developing new concepts for the design of complex thin coatings for tribological applications [1-3] and fabrication of mono-, multi-layer and superlattice architectures [4-6]. Also effective pre-coating deposition [7-11] and post-coating deposition [12-17] treatments were developed to enhance adhesion, lubrication efficiency and other specific properties. The main industrial applications of such coatings are cutting and cold forming tools [18, 19]. However, PVD coatings are increasing their diffusion also in the sector of high temperature components and, in particular, in the hot

forming of materials [20-24]. Such fields of application further to the generic wear resistance and room temperature hardness have severe materials requests in terms of hot hardness, thermal stability, thermal fatigue and oxidation resistance. Furthermore, specific operating environments such as the forming of metal alloys from liquid or semi-molten state are imposing on coatings severe chemical aggression. This is the case of casting technologies and among the others, of die-casting of aluminum alloys. Actually such alloys are particularly aggressive in the liquid state [25, 26] due to a complex mix of degradation mechanisms, i.e. thermal fatigue, corrosion/soldering and erosion by hard particles and high velocity liquid fluxes. Such harsh operating environment results in frequent requests of dies re-working, with the consequent downtime of the fabrication lines. As a consequence, despite of the related initial high investment cost advanced surface modifications technologies are becoming industrially attractive for such sectors [27]. Therefore,, many coatings are proposed on the market and extensively studied by researchers [28-32] for the protection of dies surfaces. Nevertheless, the actual service life of surface modified dies is limited by the reliability of the coated system developed. This parameter is somehow difficult to predict, since it is influenced by many factors, e.g. number of surface modified layers, layers interfaces, coatings constitution and architecture, defects introduced into the coating by the deposition technology, etc. The studies devoted to investigate the influence of such parameters can be classified as field or simulated laboratory studies. The former studies apply field tests which offer the opportunity to use close to service operating conditions, but are focused on performances rather than on failure initiation and development modes [28, 31, 33]. The latter studies use simulated conditions, but guarantee very good control of operating parameters. Some of these investigations are performed using continuous dipping conditions [30, 34, 35], others simulating the die casting thermal cycling, but without the contact with the molten metal [11], and few others applying the cyclic contact with molten metal, but avoiding the use of die lubricant or of internal cooling circuits [29, 36]. As a consequence, even for simple and widely used coatings (e.g. CrN) few systematic studies on coatings failure mechanisms in die casting conditions are given in literature [37].

This paper reports the results of a study on failure modes of CrN and ZrN monolayer coatings using cyclic immersion tests in molten aluminum alloy, using both die lubricant additions and internal cooling circuit. Such coated systems studied are commercially proposed for the protection of dies in the aluminum alloy die casting technology. The coated samples were periodically inspected, monitoring the failure initiation modes and progression as far as the number of total immersions increases. The progression of thermal cracking, corrosion and soldering was evaluated with Scanning Electron Microscopy (SEM) and Energy Dispersive Spectroscopy (EDS) analysis. A detailed description of the proposed failure modes for both coating is given. Additionally, quality assessments of coated systems were performed through nanohardness tests at different loads and SEM in the as deposited state.

2 Experimental materials and methods

The substrate material used for this study is an AISI H11 steel produced by vacuum melting and re-melting technologies, being its chemical composition reported in **Table 1**. The samples used for the major part of the research are hollow cylinders closed at one edge by a hemispherical cap (**Fig. 1a**). Opposite to such cap the cylinder has a protruding part with a hole through which the sample can be fixed at the cyclic immersion in molten metal test rig. During the test in the central cavity of the sample a stainless steel cooling channel within which thermoset water circulates is placed (**Fig. 1b**). Such cooling circuit is in close contact with the inner wall of the

sample cavity and allows keeping the sample core temperature low even when it is immersed in the molten metal. By this way a steep temperature gradient is generated throughout the sample wall during the hot stage of the cycle and a higher cooling rate is provided during the cold stage of the cycle itself. More details on such test are given below.

Table 1 Nominal chemical composition of AISI H11 [wt%].

C	Si	Mn	P	S	Cr	Mo	Ni	V
0.39	0.97	0.43	0.015	0.006	5.01	1.14	0.21	0.35

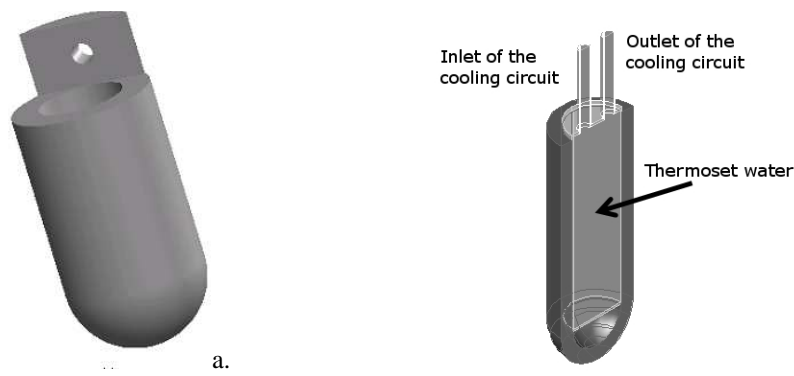


Fig. 1 Hollow cylinder sample used for the cyclic immersion in molten aluminum alloy (a); details of the sample inner cavity and of the internal cooling circuit (b)

The samples have an outer diameter of 33 mm, an inner diameter of 20 mm and a total length of 70 mm. Their fabrication cycle includes gross machining, vacuum heat treating, fine grinding and surface finishing. Details of the heat treatment are the following: austenitizing at 1000°C - quenching with 5 bar nitrogen flow - first tempering at 550°C - second and third tempering at 595°C to reach 44-45 HRC. The final surface finishing was performed manually with SiC abrasive papers (up to 1000 grit) moving the paper in the longitudinal direction, i.e. the injection/ejection direction of sample into the molten aluminium alloy.

Onto the AISI H11 samples two different ceramic monolayer coatings (CrN, ZrN) were deposited through Arc-DC-PVD techniques, using a PLATIT PL-55 unit equipped with rotating cathodes. The deposition of such coatings were carried out using pure Cr and pure Zr cathodes respectively, 5×10^{-2} mbar as chamber pressure during the deposition and 70 V as bias voltage. During each deposition run small test coupons were introduced into the chamber, to specifically study morphology, thickness, hardness and reduced Young's Modulus of the deposited coating. The overall thickness of the two coating grades is ca. 4 and 8 μm for CrN and ZrN, such values being determined through ball crater indentation test. Scanning Electron Microscopy (SEM) and Energy Dispersive Spectroscopy (EDS) analysis (LEO 1450VP + Oxford microprobe) and nanohardness measurements (MTS Nanoindenter XP) using a Berkovich indenter were performed. Nanohardness tests were carried out applying different loads, 100, 50 and 20 mN, with a loading rate of 1 mN/s.

Finally, the coated cylindrical samples were subjected to a cyclic immersion test in molten aluminum alloy. This consists in a special test rig (**Fig. 2**) where the sample is placed on a sample holder and immersed alternatively into a molten aluminum alloy bath, hot stage, and a

cooling bath made from water plus die casting lubricant, cold stage [38, 39]. Two samples per coating grades were used for this paper. The aluminum alloy used for the test was the AlSi8CuFe, being the set temperature for the molten bath $680\pm 10^\circ\text{C}$ as periodically measured by k-type thermocouples. A commercial die lubricant, Baraldi FD/1 was used to limit the aluminum alloy build up on samples. The immersion time in both the baths was 4 s, which was found by preliminary trials to be sufficient to provide the sample surface a temperature which varies between ca. 100 and 530°C . This temperature range is reasonable if compared to the typical die casting dies surface thermal cycles evaluated in industrial environments and reported by other authors [40, 41]. The maximum number of cyclic immersions achieved in the test was 20000 for all coating grades with a periodical inspection frequency ca. every 2500 cycles. The evolution of thermal damages, i.e. cracking, delamination and soldering, were investigated through SEM. Prior to such inspection, the sample surface was cleaned into boiling NaOH solution to remove the solidified Al/die lubricant residuals.

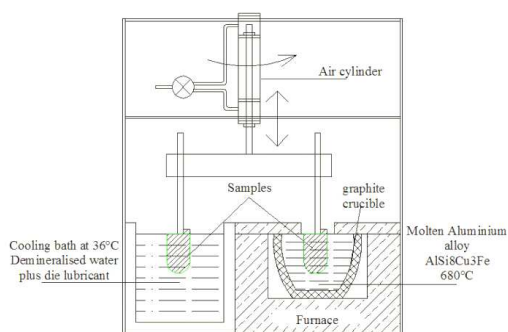
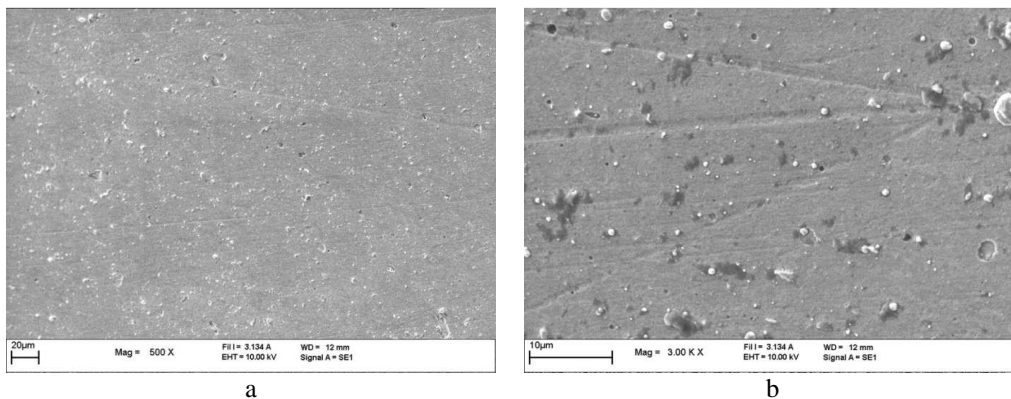


Fig. 2 Cyclic immersion in molten aluminum alloy test rig

3 Results

The surface morphology of the two studied coating grades in the as-deposited state is reported in **Fig. 3**. In both coatings top surfaces are characterized by porosities and droplets or macroparticles, which are typical features of arc deposited coatings. As far as a qualitative evaluation of droplets density and maximum dimension is concerned the levels of both these parameters result to be slightly higher in ZrN than in CrN (**Fig. 3a and c**). On the contrary, as far as the porosity is concerned, the density and average dimension of pores are very similar on both coating grades (**Fig. 3b and d**).



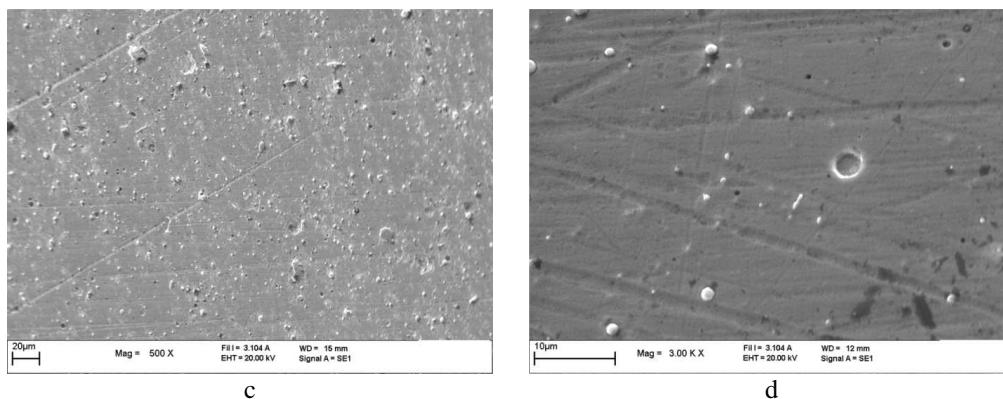


Fig. 3 Morphology at different magnifications of (a), (b) CrN and (c), (d) ZrN coatings as deposited; SEM images in secondary electrons mode.

Table 2 reports the mechanical levels recorded for the two coating grades in the nanoindentation tests. Hardness (H) and reduced Young's Modulus (E) are indeed higher for ZrN than for CrN. Such good mechanical properties are not necessarily positive in the specific application of die surface, i.e. in the prevention from damages provided by molten aluminum alloy contact, as discussed later.

Table 2 Nanohardness (H) and reduced Young's Modulus (E) data for the two coating grades.

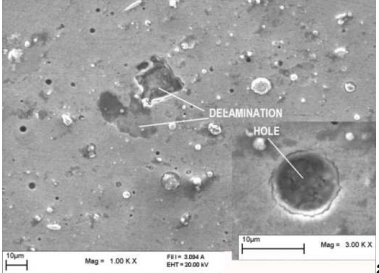
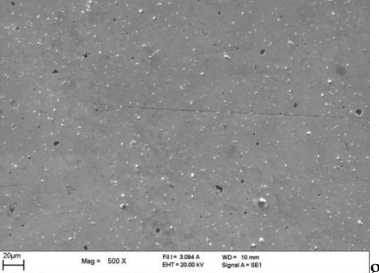
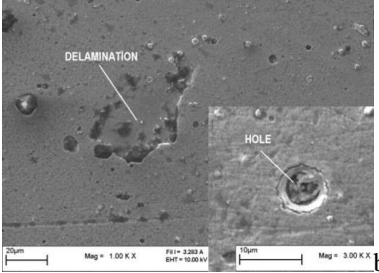
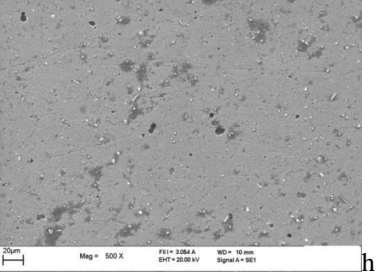
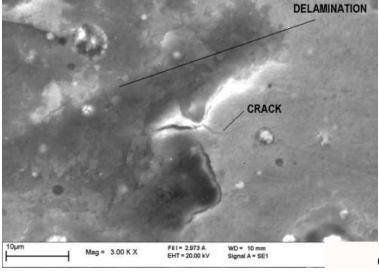
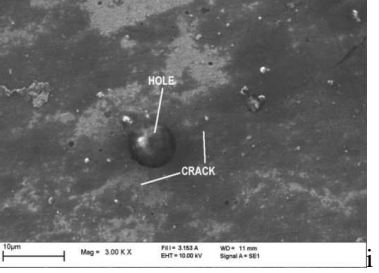
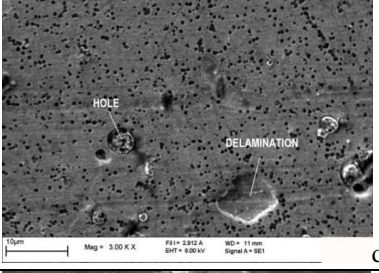
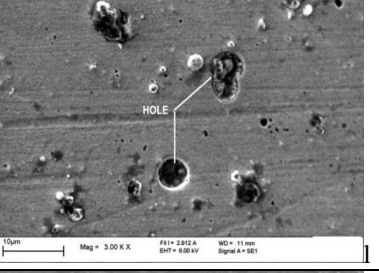
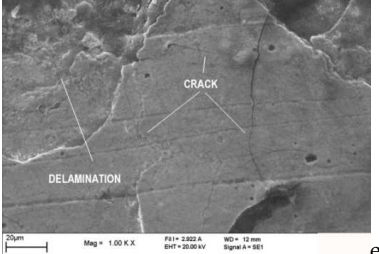
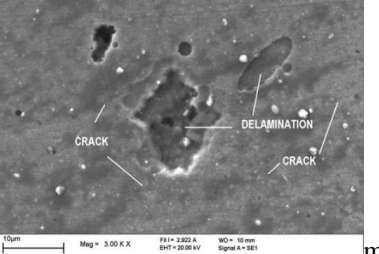
Coated System	E [GPa]	St. Dev. [GPa]	H [GPa]	St. Dev. [GPa]	Max displ. [nm]
AISI H11 + 4 μ m CrN	270	19.49	18.7	2.61	412.50
AISI H11 + 8 μ m ZrN	349	38.3	27.5	3.10	345.32

Fig. 4 reports digital photos taken during visual inspections of samples of the two coating grades at periodic inspections. Both CrN and ZrN rapidly changed their macroscopic aspect. Actually, CrN coated samples early changed their color from light to dark grey, being however the sample appearance very uniform at each inspection step. On the contrary, at least half of the length ZrN coated samples markedly changed its appearance just after 2500 cycles. After 7500 cycles the whole surface of the sample had changed its coloration from pale yellow to light grey. For both coating types the change in color has to be reasonably caused by surface oxidation, which reduces their ability to reflect light. Thus, one can preliminary guess that the ZrN exhibited a more marked tendency to oxidize with respect to CrN. Moreover, from the observation of ZrN coated samples, there is a clear evidence that the samples are not uniformly exposed along their axis to the operating environment, i.e. to the molten metal bath. Actually, even if the cylindrical samples surface are completely immersed into the molten aluminum alloy bath the upper half of the sample results to be not in continuous contact with the liquid metal itself. This is due to the solid scale film which covers the bath and to the meniscus that is generated between such film and the sample itself during the sample dipping. This is a known problem of the test practice and for such reason long samples are used for such test and only their bottom half (the one with the closed cap) is considered for inspection. This part of the samples is deeply and uniformly immersed into the molten metal bath.



Fig. 4 Macroviews of the inspection on the CrN and ZrN coated AISI H11 samples at different steps of the cyclic immersion test.

Fig. 5 reports the results of SEM analysis on samples subjected to the cyclic immersion test. The overview of coatings behavior evidences different evolutions of damages on the two coating grades. Such behavior is deeply discussed in next section.

Number of cycles	ZrN coated AISI H11	CrN coated AISI H11
2500		
5000		
7500		
10000		
15000		

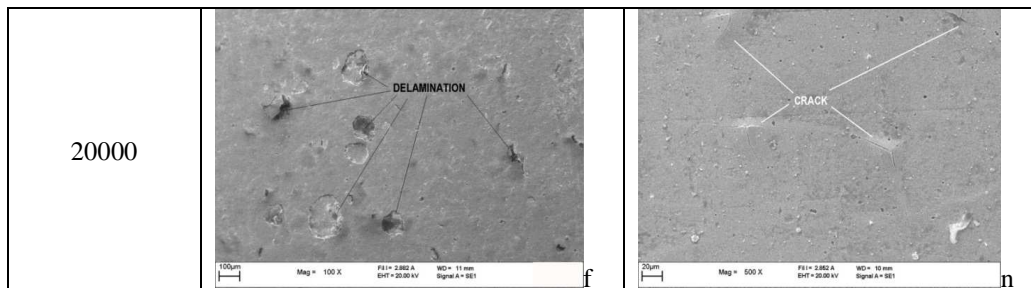


Fig. 5 SEM images of the coated surfaces subjected to cyclic immersion in molten aluminum alloy.

ZrN coating exhibits large delaminated areas and many corrosion pits just after 2500 immersion cycles (**Fig. 5a**). The so called corrosion pits are localized circular areas where the coating has failed (see small panels in **fig. 5a and b**). The typical dimension of such pits is ca. 10 μm . Conversely, delaminated areas are irregular and wide regions where the coating was removed from the substrate (see large panels in **fig. 5a and b**). The typical dimension of such areas is tenths of micrometers. The number and extension of such damages increase for ZrN coating along with the number of total immersions. At higher immersion cycles lateral cracks starts to be visible (see **Fig. 5c**) from the irregular boundaries of delaminated areas. Such cracks propagate parallel to the surface throughout the coating thickness. At 10000 cycles the density of corrosion pits is markedly increased (**Fig. 5d**). In particular, a great number of small pits (i.e. few micrometers) are visible at this stage of the test besides to the large isolated pits (i.e. tenth micrometers) which were already observed in earlier stages. At the same time the amount of delaminated areas continues to increase. Upon a further increase in the immersion cycles, macroscopic damages are observable: delaminated areas result to have average lateral dimensions of hundred micrometers (**Fig. 5e**). Also their number is highly increased (**Fig. 5f**). Long lateral cracks connecting different delaminated areas are also now visible (**Fig. 5e**).

The evolution of damages occurring on CrN is similar to that so far described, but with a reduced tendency to form large delaminated areas and with a reduced amount of corrosion pits generated (**Fig. 5g and 5h**). Actually, for less than 10000 immersion cycles although corrosion pits on CrN coated samples are present, they increase very slowly both in number and in lateral dimensions (**Fig. 5i**). For more than 10000 immersion cycles, also such coating exhibits a marked increase in the corrosion pits formation with also some isolated pits coalescence (**Fig. 5l**). Nevertheless, the density of corrosion pits at 10000 cycles on CrN is rather lower than on ZrN (**Fig. 5d and 5l**). This can be linked to the qualitative estimation of droplets density, which was assumed to be lower in CrN than in ZrN. Particular features which were in turn detected on cycled CrN coatings are radial cracks propagating from the edges of corrosion pits (**Fig. 5i**). Such cracks propagate and connect neighboring pits (**Fig. 5m**), but although they run very long, they do not provoke extended coating delaminated areas (**Fig. 5n**). Average extension of delaminated areas in CrN after 15000 immersion cycles is somehow comparable to that observed in ZrN between 2500 and 5000 cycles.

Finally, transverse section analysis of the two coated systems at the end of the test (**Fig. 6**) clearly evidences the different types of damages provided to the two coating grades. Actually, in ZrN after 20000 immersion cycles extended delamination throughout the coating thickness were observed. On the contrary, in CrN mainly thermal cracks transverse to the coating were observed

after 20000 cycles. It is worthwhile to note that in **Fig. 6a** delamination in ZrN is not complete, meaning that the steel substrate was not yet reached by the molten aluminum alloy. In this case delamination occurred due to coating de-cohesion. Furthermore, thermal cracks in CrN do not propagate straightly normal to the surface, but they do present some deviation as they are produced by a thermal fatigue process (**Fig. 6b**).

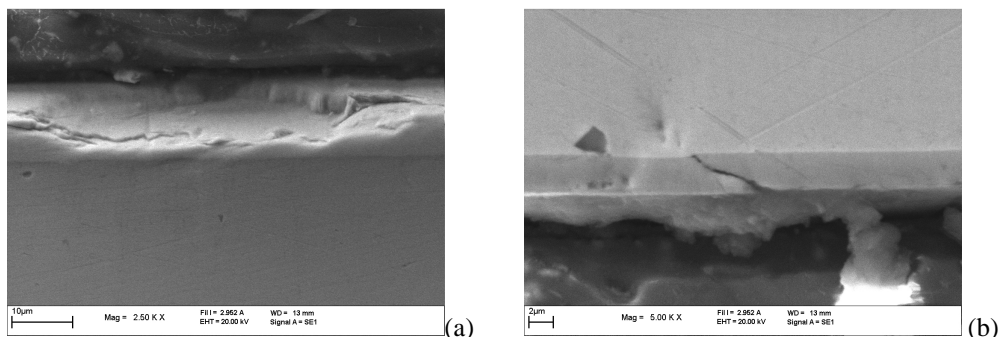


Fig. 6 SEM images of the transverse sections of (a) ZrN and (b) CrN after 20000 immersion cycles into molten aluminum alloy.

4 Discussion on coating failure modes

The description of the mechanisms proposed for the formation of damages in ZrN coated samples is given below. In an early stage (i.e. less than 10000 cycles), relatively few corrosion pits form on the coating surface. It is generally recognized that nitride coatings are not subject to direct corrosion from the contact with molten aluminum alloy [35, 42]. Nevertheless, the sources for the formation of corrosion pits are coating defects, either pores or droplets: in the first case the substrate is a priori uncovered by the coating, whereas in the latter it can be rapidly exposed by the removal of droplets, caused by the tangential forces applied from the aluminum alloy flux and by the alternated cycles of thermal dilatation/contraction. At such locations corrosion and soldering of the steel substrate occurs and progressively expands laterally below the coating along the coating/substrate interface. The steel substrate corrosion is generally accepted to be caused by the formation of intermetallic phases [43], but this aspect was not addressed by the current paper. As a consequence, in an annular area around the original coating defect the coating is not more supported by the substrate and collapses through the formation of circumferential cracks (see small panels in **Fig. 5a and b**). The number and lateral dimensions (some tenths of micrometers) of such pits appears to stabilize for immersion cycles lower than 10000. The fact that corrosion pits are formed very early, but they do not significantly increase in number can be explained by the following proposed model. The formation of such pits is mainly governed by the presence of pores, which directly put in contact the molten alloy with the steel substrate. Another possible formation mechanism is that the origin of corrosion pits is provided by droplet sites. Such process is indeed slower because it involves the progressive cracking of coating layers up to the complete exposure of the substrate to the operating environment. Independently by the formation source, the limited lateral expansion of the corrosion pits gives clues to the fact that, once the corrosion of steel substrate is initiated, it propagates preferentially towards the steel core rather than along the coating/substrate interface. At this stage no radial cracks were observed at the edges of corrosion pits. Other authors [36]

proposed that the corrosion pits forms mainly at coating thermal cracking sites. Such cracking was indeed observed later in our tests and is described below, but the circular shape of the corrosion pits and the absence of thermal cracks let us to conclude that in our case they form preferentially at coating defects sites.

The formation of delaminated areas is mainly related to a coating/substrate interface de-cohesion which initiates at the corrosion pits. Actually, at such sites the coating/substrate interface is weakened by corrosion effects as previously described. This can introduce a sort of pre-cracking of such interface. At the same time during hot and cold cycles of the immersion cycle test compressive and tensile stresses are alternatively applied through the coating and across the coating/substrate interface. These are thermal stresses caused by the mismatch in terms of coefficients of thermal expansion between the thin ceramic coating and the steel substrate. The repeated application of thermal cycles finally leads to the formation of cracks, which releases the high residual tensile stresses accumulated by the coated systems. Such cracks can be nucleated either at the coating surface or at the coating/substrate interface. In the case of ZrN the previously mentioned pre-cracked coating/substrate interface favors the initiation of de-cohesion at corrosion pits edges. This progressively spalls off the coating and at a certain critical stage two or more neighboring coating de-cohesion fronts meet and cause the portion of the coating which lies between them to delaminate, resulting in the large delaminated areas. However, it was also possible to note that partial delamination of coating sometimes occurred as a consequence of de-cohesion of coating within its thickness (**Fig. 6a**). Such type of delamination starts again from corrosion pits, but do not directly expose the steel substrate. This damage is probably generated by the fact that internal defects are present also within the coating thickness.. Like in complete delamination, neighbor corrosion pits can then be linked thus generating large delaminated areas.

As a consequence of their formation process, i.e. linking of randomly dispersed corrosion pits, partial or complete delaminated areas have irregular shapes (see large panels in **Fig. 5a and 5b**). Therefore, at sharp edges of such regions radial cracks are nucleated and propagated horizontally through the coating (**Fig. 5c**), thus further extending the delamination.

At a later stage of the test, i.e. after 10000 cycles of immersions, ZrN exhibits a much diffused pitting effect with even coalescence effects of neighboring pits (**Fig. 5d**). The multiplication of corrosion pits can be explained by the fact that the incubation time for the cracking around droplets and their complete removal is now completed and at this stage all the coating defects (both pores and droplets) are completely active in giving pits formation. As a consequence of the increased number of corrosion pits the delamination and the following edge cracking are exalted leading to an extended coating removal (**Fig. 5e and f**). Large delaminated areas expose the steel substrate to molten aluminum alloy contact and corrosion, with following soldering and solidified aluminum build up.

The observations performed on CrN coated samples subjected to the cyclic immersion test suggest that the failure mode for such coating is slightly different from that proposed so far for the ZrN. Actually in this case the proposed descriptive model is the following. Initially corrosion pits are formed like in ZrN. However, as a consequence of the reduced original pores density in CrN a smaller amount of corrosion pits is generated. Later on from such corrosion pits sites thermal stresses in CrN coated samples are released by the formation of cracks at the coating surface. Such cracks nucleate at the coating surface and propagate transversally through the coating. This propagation is driven by a thermal fatigue process which provides cracks deflections (**Fig. 6b**) and can be therefore considered to be slow. The very interesting aspect of

the damaging mechanism in CrN is that coating/substrate de-cohesion does not occur. To explain this, it is necessary to consider that CrN is a markedly less hard than ZrN and is therefore able to better accommodate the thermal coefficient mismatch between coating and steel substrate, thus reducing the stresses acting at the coating/substrate interface. Of course, the lower hardness of CrN can also explain the fact that coating cracks are visible earlier in such coating than in ZrN. Although this is negative for the quality of cast parts, such early and diffused cracking of CrN coating can provide a sort of stress release of the whole coated system. On the contrary, this results also in the presence of new possible nucleation sites for corrosion pits formation (thermal cracks sites). However, through such mechanisms in CrN the protection of the steel substrate is removed only in localized areas, i.e. around pores, droplets or thermal cracks, whereas in ZrN is removed in large portions of the surface, i.e. delaminated areas. This leads to the conclusion that in this study CrN coating resulted to be more effective than ZrN at least in terms of steel substrate protection.

5 Conclusion

A comprehensive study of failure mechanisms of CrN and ZrN coating in cyclic contact with molten aluminum alloy was performed using a simulating test. The morphology and mechanical properties of coatings were also studied. The morphological features as well as the mechanical levels were discussed in terms of their influence on the performance of the coated systems in the service environment and operating conditions.

The main conclusions of the study are:

- coating defects are main sources for the formation of circular corrosion pits on coated surfaces: pores directly expose the steel substrate, whereas droplets require a certain incubation time to expose the steel substrate and to activate the corrosion mechanisms
- especially in CrN thermal cracks can also provide new sites for corrosion pits formation
- in ZrN coating thermal stresses provided by cyclic immersion in molten aluminum alloy are mainly released by cracks nucleating around the corrosion pits and propagating through the coating/substrate interface interface, with progressive de-cohesion finally resulting in extended delamination; in some cases de-cohesion of coating is also provided thus giving partial coating delamination
- in CrN coating the release of thermal stresses occurs through radial cracks which start again from the corrosion pits edges and later propagate to neighbor defects in coating; although defects on cast parts and new corrosion sites can be provided in such condition, the damaging mechanism is slower and provide longer substrate protection, if compared to ZrN.

Actually, both the failure modes of coatings ultimately leads to the exposure of steel substrate to the operating environments, but the formation of large delaminated areas in ZrN is rather fast, thus exposing large portions of the steel substrate to molten Al alloy corrosion. On the contrary, CrN fails by localized thermal cracking, which is a slow process and finally exposes limited portions of the steel substrate. As a further confirmation to this, it can be considered that marked coating damages were assessed for less than 5000 immersion cycles in the case of ZrN whereas between 10000 and 15000 cycles in the case of CrN.

References

- [1] P.H. Mayrhofer, C. Mitterer, L. Hultman, H. Clemens: *Progress in Materials Science*, Vol. 51, 2006, p. 1032-1114
- [2] A. Matthews, A. Leyland, K. Holmberg, H. Ronkainen: *Surface and Coating Technology*, Vol. 100-101, 1998, p. 1- 6
- [3] A. Matthews, S. Franklin, K. Holmberg: *Journal of Applied Physics D: Applied Physics*, Vol. 40, 2007, p. 5463-5475
- [4] P. Eh. Hovsepian, W.-D. Munz: *Vacuum*, Vol. 69, 2003, p. 27–36
- [5] P. Eh. Hovsepian, D.B. Lewis, W.-D. Munz: *Surface and Coatings Technology*, Vol. 133-134, 2000, p. 166-175
- [6] Q. Luo, W.M. Rainforth, W.-D. Munz: *Surface and Coatings Technology*, Vol. 146-147, 2001, p. 430–435
- [7] K.-T. Rie, E. Broszeit: *Surface and Coatings Technology*, Vol. 76–77, 1995, p. 425-436
- [8] T. Wierzchon: *Surface and Coatings Technology*, Vol. 180-181, 2004, p. 458–464
- [9] B. Navinšek, P. Panjan, I. Urankar, P. Cvahte, F. Gorenjak: *Surface and Coatings Technology*, Vol. 142–144, 2001, p. 1148-1154
- [10] Ma Shengli, Li Yanhuai, Xu Kewei: *Surface and Coatings Technology*, Vol. 137, 2001, No. 2–3, p.116-121
- [11] K. Kulkarni, A. Srivastava, R. Shivpuri, R. Bhattacharya, S. Dixit, D. Bhat: *Surface and Coatings Technology*, Vol. 149, 2002, p. 171–178
- [12] I. Etsion: *Journal of Tribology*, Vol. 127, 2005, p. 248-253
- [13] T.V. Kononenko et al.: *Applied Physics A*, Vol. 71, 2000, p. 627–631
- [14] M. S. Trtica et al: *Applied Surface Science*, Vol. 252, 2005, p. 474–482
- [15] J.M. Geuß, S. Baudach, H. Sturm, W. Kautek: *Applied Physics A*, Vol. 69, 1999, p. S399–S402
- [16] A.G. Demir, B. Previtali, N. Lecis, L. Vandoni, D. Ugues: *Metallurgia Italiana*, Vol. 104, 2012, No.6, p. 15-19
- [17] L. Vandoni, A.G. Demir, B. Previtali, N. Lecis, D. Ugues: *Materials*, Vol. 5, 2012, p. 2360-2382
- [18] W. Kalss, A. Reiter, V. Derflinger, C. Gey, J.L. Endrino: *International Journal of Refractory Metals and Hard Materials*, Vol. 24, 2006, p. 399–404
- [19] I.J. Smith, D. Gillinbrand, J.S. Brooks, W.D. Munz, S. Harvey, R. Goodwin: *Surface and Coating Technology*, Vol. 90, 1997, p. 164-171
- [20] A. Raveh, I. Zukerman, R. Shneck, R. Avni, I. Fried: *Surface and Coating Technology*, Vol. 201, 2007, p. 6136-6142
- [21] H.-D. Männling, D.S. Patil, K. Moto, M. Jilek, S. Veprék: *Surface and Coating Technology*, Vol. 146-147, 2001, p. 263-267
- [22] D. Bok Lee, T. Dinh Nguyen, S. Kyu Kim: *Surface and Coating Technology*, Vol. 203, 2009, p. 1199-1204
- [23] T. Polcar, A. Cavaleiro: *Materials Chemistry and Physics*, Vol. 129, 2011, p. 195-201
- [24] L. Wang et al.: *Surface and Coating Technology*, Vol. 203, 2008, p. 816-821.
- [25] V. Joshi, A. Srivastava, R. Shivpuri: *Wear*, Vol. 256, 2004, p. 1232–1235
- [26] K. Domkin, J.H. Hattel, J. Thorborg: *Journal of Materials Processing Technology*, Vol. 209, 2009, p. 4051–4061.
- [27] C. Pfohl, A. Gebauer-Teichmann, K.-T. Rie: *Surface and Coatings Technology*, Vol. 112, 1999, p. 347-350

- [28] D. Heim, F. Holler, C. Mitterer: Surface and Coatings Technology, Vol. 116–119, 1999, p. 530–536.
- [29] C. Mitterer, F. Holler, F. Ustel, D. Heim: Surface and Coatings Technology, Vol. 125, 2000, p. 233–239
- [30] C. Mitterer, F. Holler, C. Lugmair, R. Nobauer, R. Kullmer, C. Teichert: Surface and Coatings Technology Vol. 142-144, 2001, p. 1005-1011
- [31] S. Gulizia, M.Z. Jahedi, E.D. Doyle: Surface and Coating Technology, Vol. 140, 2001, p. 200-205
- [32] M. Rosso, D. Ugues, E. Torres, M. Perucca, P. Kapranos: International Journal of Material Forming, Vol. 1, 2008, Suppl. 1, p. 1259-1262
- [33] B. Navinšek, P. Panjan, I. Milošev: Surface and Coatings Technology, Vol. 97, 1997, No. 1–3, p. 182-191
- [34] C.S. Lin, C.S. Ke, H. Peng: Surface and Coating Technology, Vol. 146-147, 2001, p. 168-174
- [35] A. Molinari, M. Pellizzari, G. Straffellini, M. Pirovano: Surface and Coating Technology, Vol. 126, 2000, p. 31-38
- [36] Y. Wang: Surface and Coatings Technology, Vol. 94–95, 1997, p. 60-63
- [37] J. Lin, S. Carrera, A.O. Kunrath, D. Zhong, S. Myers, B. Mishra, P. Ried, J.J. Moore: Surface and Coating Technology, Vol. 201, 2006, p. 2930-2941
- [38] D. Ugues, E. Torres Miranda, M. Perucca, M. Albertinazzi, M. Rosso: International Journal of Microstructure and Materials Properties, Vol. 2, 2007, No. 1, p. 99-108
- [39] E. Torres Miranda, D. Ugues, Z. Brytan, M. Perucca: Journal of Physics D: Applied Physics, Vol. 42, 2009, 105306
- [40] Z.W. Chen: Materials Science and Engineering A, Vol. 397, 2005, p. 356-369
- [41] R. Ebner et al.: *Methodology for advanced tool load analysis and lifetime prediction of tools*, In.: Proceedings of the 9th international tooling conference, Leoben, Montan universitat Leoben, 2012, p. 3-24
- [42] K.T. Rie, C. Pfohl, S.H. Lee, C.S. Kang: Surface and Coating Technology, Vol. 97, 1997, p. 232-237
- [43] V. Joshi, A. Srivastava, R. Shivpuri: Wear, Vol. 256, 2004, p. 1232–1235

Acknowledgements

As some of the results reported were achieved in the framework of the FP7 project “Multiscale Modelling for Multilayered Surface Systems (M3-2S)”, Grant No: CP-FP 213600-2 M3-2S, the authors thank the European Committee for its support. The authors wish to thank Clean NT Lab Division, Environment Park S.p.A., Bohler and Baraldi for providing the deposition system, substrate steel and die casting lubricant respectively.